

**A QUANTITATIVE TUNNELING/RESORPTION MODEL FOR THE  
EXCHANGE CURRENT AT THE POROUS ELECTRODE/BETA"-  
ALUMINA/ALKALI METAL GAS THREE PHASE ZONE AT 700-1300K**

R. M. Williams, M. A. Ryan, C. Saipetch, and H. G. LeDuc

Jet Propulsion Laboratory  
California Institute of Technology  
Pasadena, CA 91109

**AIMTRACT**

The exchange current observed at porous metal electrodes on sodium or potassium beta"-alumina solid electrolytes in alkali metal vapor is quantitatively modeled with a multi-step process with good agreement with experimental results. No empirically adjusted parameters were used, although some physical parameters have poor precision. Steps include 1) electron tunneling from the porous metal electrode surface to alkali ions at the defect block edge; 2) reorganization consisting of vibrational excitation of the surface bound alkali ions; 3) resorption of alkali metal atoms to the gas phase; 4) tunneling of electrons between alkali atoms and ions along the edge of the defect block to transfer charge away from the three-phase boundary in a random walk; and 5) surface diffusion of ions or atoms away from the defect block edge onto the spinel block edge.

The rate is increasingly dominated by the region close to the three-phase boundary as temperature increases and the rate near the three-phase boundary increases fastest, because resorption has a higher energy than reorganization. At high temperatures, surface diffusion of Na<sup>+</sup> ions from the defect block edges to the spinel block edges is responsible for an increase in the total effective reaction zone area near the three-phase boundary.

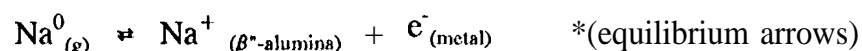
**1. INTRODUCTION AND GENERAL DESCRIPTION OF THE MODEL**

It is generally accepted that heterogeneous electron exchange electrochemical reactions exhibit high rates due to electron transfer via tunneling, but quantitative modeling of real reactions is difficult because of the complexity of the ancillary processes which precede and follow electron transfer, especially when liquid electrolytes are involved. Gurney proposed that tunneling must play an important role in electrochemical electron transfer reactions. [1] This conclusion was extended and more thoroughly treated with the work of Gerischer, and is generally presented in electrochemistry texts, but fundamental

models showing quantitative agreement with experiment are lacking. [2] Some of the problems inherent to solution electrochemistry are eliminated in developing a quantitative model of heterogeneous electron transfer reactions when solid electrolyte/solid electrode/low pressure gas electrochemical systems are investigated, since the mechanics of mass and charge transfer are somewhat simpler. However, other problems arise because an adequately precise definition of electrolyte and electrode morphology is necessary,

## 1.1 DEFINITION OF THE EXCHANGE CURRENT

The experimental exchange currents for the reduction and oxidation of alkali metal ions and atoms at porous metal electrodes on alkali metal  $\beta$ -alumina solid electrolytes (BASE) in low pressure alkali metal vapor have been evaluated over the temperature range from 700 K to 1250 K. [3-5] We define the exchange current to consist of the equal and opposite redox processes which occur at reaction sites which can contribute to a continuous dc current when the cell is perturbed from the stationary state. Then the reaction zone will be the region where the incoming and outgoing sodium atom fluxes become different when a potential is applied across the cell. If there is no effective transport mode away from a reaction site, the contribution of the exchange current at that reaction site to the dc exchange current is negligible. Local transport of ions or atoms at the reaction site may have important effects on the exchange current, if, for example,  $\text{Na}^+$  ions can diffuse rapidly on the spine] block surface between defect block edges, the effective reaction area at the three-phase boundary would be quadrupled. Note that a frequency exchange current which does not require escape of the reaction product might also be defined, and would be larger.



Measurements have been made for a variety of electrodes including Mo, Mo/ $\text{Na}_2\text{MoO}_4$ , WRh alloys, WPt alloys, and TiN on sodium  $\beta$ -alumina in sodium vapor, as well as for Mo electrodes on potassium  $\beta$ -alumina in potassium vapor. [3-6] At typical pressures of alkali metal vapor encountered in these experiments, metal electrodes have an adsorbed less-than-monolayer coverage of the alkali metal. [7] These adsorbed layers result in a substantial decrease in the work function of the electrode. [8-10] All experimental electrode performance data in this paper has previously been reported.

Measurements have been carried out in power producing alkali metal thermal to electric converter (AMTEC) cells where the anode is liquid alkali metal in contact with BASE. The impedance of the liquid metal electrode/BASE interface at high temperatures is negligible. [S, 11] The exchange current has been determined from these cells by deconvoluting the contributions of kinetics and transport from the mixed control Faradaic component of the impedance measured

as a function of cell potential. [5] We have reported exchange currents for most of the electrodes described above either referenced to the saturated vapor pressure of the alkali metal, or using an empirical parameter, roughly independent of temperature, which relates the exchange current at any alkali metal vapor pressure to the collision rate of alkali atoms in the vapor with the electrolyte surface. [3,5] The temperature dependence has been fit to a semi-empirical model which relates it to the collision, or adsorption/resorption rate of the alkali metal with the BASE surface, multiplied by an empirical constant. [3] The observation that the exchange current was proportional to the alkali metal gas collision frequency, with the empirical parameter nearly independent of temperature and pressure, suggested that the exchange current could be modeled fairly simply and formed the basis for the model developed in this paper. [3] While differences exist among the results from various electrode materials, the exchange currents of oxide-free metallic electrodes show both a relative] y narrow distribution at the same temperature, as well as similar temperature dependence. There is a decrease in observed exchange currents for some electrodes at high temperature as grain-growth in the porous metallic electrode occurs, reducing the length of the three-phase boundary between electrode, electrolyte, and vapor. [12] This observation indicated that the reaction zone was confined to a region quite close to the three-phase boundary, with a width much less than 0.25 $\mu$ m, a radius of grains or pores in Mo electrodes at which further increases in grain and pore size significantly reduced measured exchange currents.

## 1.2 DESCRIPTION OF THE MODEL

This paper will discuss the microscopic mechanisms which account for the observed electrode kinetics of the alkali metal coated porous metal electrode/p"-alumina/alkali metal vapor three-phase interphase region.

We describe a detailed model] without empirically derived parameters. This model is constructed using physical parameters which are known or can be estimated (sometimes with poor precision) with some reliability, and includes only physical processes for which there is substantial evidence. For convenience, the discussion of reaction steps generally will describe the cathodic reaction, an electron tunneling from the Mo electrode to a  $\text{Na}^+$  ion, with eventual resorption of a sodium atom, but apply equal] y well to the reverse, anodic reaction. Asymmetry will only enter the treatment when transport effects are discussed. At zero volts, all of the reverse steps are equally likely, and generally K may be substituted for Na, or W or other metal electrodes may take the place of Mo, with change in the work function. The morphological parameters for the electrode and the exchange current dependence on temperature are well characterized only for 0.5  $\mu$ m thick molybdenum electrodes. The basic model describes the reaction as a four step sequence: (1) diffusion of  $\text{Na}^+$  ions to the

reaction site; (2) stretching of the  $\text{Na}^+$  ionic bond with the  $\beta$  "-alumina surface to reach a configuration suitable for accepting an electron to form a surface bound  $\text{Na}^0$  atom; (3) electron tunneling from the Mo electrode to the ions; and (4) desorption of  $\text{Na}^0$  atoms weakly bound at the reaction site on the  $\beta$  "-alumina surface. The first two steps have little effect on the rate, as they are faster than the third step at the temperatures under consideration, and neither of these steps has any dependence on position. The tunneling step is very fast close to the three phase boundary line, but is slow at distances of several nm from the three phase line, and hence defines the effective reaction area,

The basic model has no adjustable empirical parameters and reproduces the temperature dependence, in the range from 800 K to 1200 K, of the exchange current of the porous Mo electrode,  $\text{Na}^0$  vapor/ $\text{Na}$ - $\beta$  "-alumina system very well. The exchange current varies by a factor of about 100 over this temperature range. We use geometric mean values instead of the most favorable values of these parameters. We evaluate two additional mechanisms, including electron hopping along the defect block and ion/atom mobility on the spinel block surface. Additional experimental data will be required to determine what changes in the model are justified to improve agreement between experiment and calculation.

#### 1.4 ELECTRODE MORPHOLOGY

Three morphological parameters directly affect the reaction rate. These are the length of the three-phase boundary, the fraction of the BASE surface which is electrochemically active, and the contact angle between the electrode and the BASE. The reaction area depends linearly on both the length of the three-phase boundary and the fraction of BASE surface composed of electrochemically active [hk0] crystallite faces. The reaction area also depends on the contact angle between crystallite grains of the porous electrode and the solid electrolyte, because the area of the electrode surface from which electrons can tunnel to  $\text{Na}^+$  ions on the surface of defect plane blocks of the BASE decreases as the angle between the surfaces increases. The length of the three phase line and the contact angle have been characterized by scanning electron microscopy. We have previously reported surface decoration experiments which were used to attempt to measure the fraction of BASE crystallite grains which are electrochemically active in typical ceramic, with results from 5-30%. [3] The crystal structure of alkali  $\beta$  "-alumina is well known, with quasi-two dimensional defect blocks containing conducting ions isolated by spine blocks.

#### 1.3 BASIC ASSUMPTIONS

The work function of the porous metal electrode is the height of the energy barrier for tunneling from the electrode to the sodium ion on the BASE surface.

Extensive measurements have been made of the work functions of Mo and W, with alkali metal sub-monolayer films. We use the work function for Na on W since that of Na on Mo is less well characterized, and the differences should be minor. Sodium depresses the work function somewhat less than the heavier and more electropositive alkali metals, but some measurements are available, [9,10]

A surface structure and sodium ion population for the defect block is assumed which is similar to the known structure in the crystal interior, although some simplification of distribution of sodium ions to a regular period is made. Electron migration away from the three phase region occurs by a random walk, and both the rearrangement of sodium ions prior to tunneling from sodium atoms and the desorption of sodium atoms are activated processes. The rate of desorption is about 3000 times faster at 1300K than at 700K, while the sodium ion stretch required for rearrangement is about 30 times faster at the higher temperature, calculated from the known desorption energies of sodium ions from sodium beta alumina crystals. [15] The tunneling rate is not very temperature dependent, so the number of hops is the average residence time of the sodium atoms before desorption times the hopping frequency, so that about 100 times more hops occur at 700K than at 1300K. The addition of the electron hopping mechanism brings the calculation to within a factor of two lower than experiment at 700K and about a factor of three lower at 1250K. Its poorer agreement at high temperature suggests that a weakly activated transport process such as surface diffusion of sodium ions to the spinel block surfaces between the defect blocks, or sodium atom transport along Me/p  $\gamma$ -alumina grain boundaries to the Mo grain edge may be responsible for the remaining discrepancy.

We make the assumption that reactive surface grains are oriented with [001] or [hk0] faces exposed, because grain fracture with any component along the basal plane [001] results in predominate  $\gamma$  basal plane surfaces. Defect blocks which contain the conducting ions are equally distributed on any [hk0] surface, and [001] faces are expected to be electrochemically inactive. We then calculate the defect block density on the BASE surface. The calculations and description are referenced to one isolated defect block in order to describe the microscopic process as accurately as possible.

The rate of the  $\text{Na}^+$  diffusion step to the reaction site is estimated from the conductivity of  $\text{Na}^+$   $\beta$ -alumina single crystals at high temperatures. We assume that the structure of the defect block at the surface is not substantially modified, and that the  $\text{Na}^+$  ions are restricted to the defect block surface. There appears to be no reported evidence about diffusion rates of  $\text{Na}^+$  across the spinel block surface. The thickness of the defect block (>.216 nm) is somewhat greater than the diameter of the  $\text{Na}^+$  ion, because some ions are above and some are below the plane of the center of the defect block, and the BASE defect block structure readily accommodates the larger  $\text{K}^+$  ion (.266 nm) with slight c axis expansion.

The spine] block is 0.85-0.90 nm thick, and migration of  $\text{Na}^+$  by less than 0.5 nm onto spine] block surfaces could quadruple the rate if surface migration over this distance is competitive with the resorption rate of the alkali metal from the defect block. Surface decoration experiments indicate that the BASE surface is divided into inactive and active grains, but these experiments were conducted at lower temperatures; additional information provided by the decrease in the exchange current with Mo grain-growth showing that  $\text{Na}^+$  ion diffusion over distances  $> 0.1 \mu\text{m}$  onto [001] grain surfaces is not important. The calculation assumes electron transfer only to  $\text{Na}^+$  ions on defect block surfaces. Rearrangement of bond distance and geometry when electron transfer takes place is expected to be very rapid, but may play a role in limiting electron transfer by a series of hops between the electrode and sodium ions outside of the range of high probability direct tunneling. Because the entire electrolyte surface is exposed to collisions with sodium atoms, there is no reason to expect concentration gradients of adsorbed alkali atoms under steady state conditions, and even at non-zero dc currents the adsorbed sodium atom concentration on the BASE surface will tend to equilibrate through the gas phase.

The resorption rate is taken to be equal to the collision rate of alkali metal vapor in equilibrium with the liquid alkali metal, implying a sticking coefficient of 1.0, and complete reversibility. Wetting characteristics of liquid sodium on BASE provide qualitative information about the surface energy between liquid sodium and BASE. Liquid sodium does not wet BASE at low temperatures, but does wet it at temperatures above about 673 K.[12] The low temperature behavior may be affected by surface contamination. We have found that liquid sodium can be poured from BASE tubes at about 400K without leaving a sodium film, following long-term high temperature operation, but Na films form at higher temperatures. This moderate wetting suggests that the interracial free energy between liquid sodium and BASE is probably positive, but smaller than the surface free energy of sodium, at least at higher temperatures. A molecular orbital calculation of the binding of a single sodium atom to an  $\text{AlO}_3^{2-}$  cluster in the environment of an ionic solid has been carried out and results indicate that if appropriate charge compensation occurs, atomic sodium will bind to a  $\beta$ "-alumina surface, but that because  $\beta$ "-alumina has no low-lying unoccupied electronic levels, the sodium 3s electron will remain associated with the sodium atom. [14] This suggests that the adsorption of a sodium atom can not be considered to involve ionic, covalent, or any other strong chemical bond. We cannot estimate the binding energy of a sodium atom or a sodium layer on a BASE surface more precisely with currently available data. We therefore use an approximation to the binding energy of a sodium atom at the surface of the bulk, with its number of nearest neighbors reduced from about 12 to about 9, recognizing that this value is still possibly too large, especially at low pressures and coverages in which the adsorbed layer does not have the characteristics of bulk liquid sodium.

### 3. MODEL DEVELOPMENT AND RESULTS

The microscopic model for kinetics and transport in AMTEC electrodes requires understanding of the dependence of electrode operation parameters on electrode and interface morphology, as well as experimental characterization of these parameters with respect to temperature and other variables. This model contains significant simplifications, but it begins to put AMTEC electrode mechanistic phenomena at a molecular level on a more quantitative basis.

The Faradaic impedance of the liquid sodium electrode/Na-BASE interface is negligible. As a result the impedance of AMTEC cells contains significant contributions from BASE and lead ohmic resistances and small inductances from the lead configurations, and a major Faradaic impedance only from the porous electrode/BASE/vapor interphase region on the low pressure side of the AMTEC cell. Measurements performed on oxide free thin ( $0.5\mu\text{m}$ ) Mo and ( $1.0\text{--}1.5\mu\text{m}$ ) W/Rh and W/Pt electrodes have shown fairly consistent exchange currents which are proportional to collision rates of Na gas at the interface over several hundred K. [3] Electrodes containing metal oxide phases exhibit both fairly high ionic and electronic conductivity, and their exchange currents are often significantly higher, by a factor of 5 or 6, than those of oxide-free metal electrodes. The transfer coefficient,  $\alpha$ , has been determined to be close to 0.5 based on high quality impedance data on mature electrodes at high temperatures,  $T > 1100\text{K}$ , and no systematic deviation from this value is observed on cooling, although the scatter in derived values increases substantially. This argues for a simple, symmetric reaction for  $\text{Na}^+ + \text{e}^- \rightarrow \text{Na}$ .

#### 3.1 Morphology of the Three-Phase Interface

For high performance  $0.5\mu\text{m}$  thick Mo electrodes, using data for grain size, void area from scanning electron microscopy (SEM) of Mo electrodes, initially deposited as sputtered films, following operation in AMTEC cells or sodium or potassium vapor exposure cells at temperatures from 1150–1200K and operation times of >25 hours, the approximate electrode grain/BASE contact angle is estimated at 60 degrees, the length of the three-phase boundary,  $l_3$ , is estimated to be  $3 - 6 \times 10^6 \text{ m per m}^2$  of projected geometric electrode area,  $A_{\text{GEOM}}$ . The total three-phase boundary length is the product of the number of grains per unit area and the length of the boundary of a single grain.

A somewhat fuzzy experimental upper limit on the extent of the reaction zone can also be established, since the grain-growth of thin Mo electrodes at  $\sim 1200\text{K}$  leads to a drop in the observed exchange current as the Mo grain size increases from approximately  $0.5$  to  $1.0\mu\text{m}$  and pores in the Mo film of  $0.5$  to  $5.0\mu\text{m}$  diameter appear. Therefore we can expect that the upper limit of

the extent of the reaction zone is less than 0.25  $\mu\text{m}$ , the radius of smaller pores, and the lower limit is on the order of about 1.0 nm, since a smaller reaction zone could not possibly account for the observed rate since too few collisions would occur in this area.

Estimates of the macroscopic fractional reactive surface area of a BASE ceramic surface,  $F_{\text{EDGE}}$  range from 5 % to 30% of the total BASE surface area,  $A_{\text{BASE}}$ , which in turn is several times the projected surface area,  $A_{\text{GEOM}}$ , because the ceramic has a bumpy, irregular surface. These estimates are based on low temperature surface decoration experiments, and scanning electron microscopy, for  $F_{\text{EDGE}}$  and  $A_{\text{BASE}}$ , respectively. [3]

We adopt a microscopic model in which one defect block,  $3 \times 10^{-10}$  m in width, extends away from the three-phase boundary, as shown in **Figure 1**. We arbitrarily choose a perpendicular orientation from the three phase line, but all possible orientations exist and the density of defect blocks on  $\{hk0\}$  planes as a function of distance from the three-phase line is uniform averaged over a large area. We calculate how many defect blocks oriented perpendicular to the three - phase line would be required to account for all the defect block area per square meter of BASE surface coated with porous electrode. Calculations are carried out in cylindrical coordinates in which  $x'$  is the distance from an area element of a defect block along a line normal to the electrode and  $r$  is a radial coordinate on the electrode surface away from the intersection of the normal. The contact angle between the electrode and the BASE is  $\theta$ . For acute angles, the normal to the electrode surface is above the three-phase boundary by a distance,  $h(x)$ , such  $h$  completes the right triangle with  $x$  and  $x'$ . For values of  $r > h$ , only the portion of the ring of width  $dr$  with an angle above  $\theta$  and below  $2\pi - \theta$  measured from  $h$  is electrode area which contributes to the tunneling current,

If only the defect block edges are reactive fractional microscopic reactive part of the three phase boundary is in the range of 0.04 to  $1.0 \times 10^6$  m/m<sup>2</sup>. The model is developed for one defect block for clarity and multiplied by  $6.7 \times 10^{14}$  defect block edges/m<sup>2</sup> for a typical Mo electrode.

### 3.2 Description of Collision Rate of Na Atoms

The collision rate for sodium atoms with the surface come from the kinetic theory of gases, since gas pressure is due to momentum exchange when gas molecules strike a surface. At equilibrium, we assume the sticking coefficient is 1.0, but that every adsorbed atom from a collision is balanced by a desorbed atom.

$$x_{\text{Na}} = P/[2 \sqrt{m_{\text{Na}} k_B T}] \quad [\text{Eq. 2}]$$

The collision rate per square meter of surface exposed to sodium vapor,  $X_{\text{Na}}$



is  $6.888 \times 10^{23} (P/\sqrt{T}) \text{ m}^{-2} \text{ s}^{-1}$ . If we assume that the collision rate controls the reaction rate, as is suggested by the similar type in the temperature dependence of the collision rate and the exchange current, but assume the reaction is limited to defect block surface close to the three phase boundary, we can calculate a semi-empirical rate which agrees moderately well with experiment for a reaction zone width consistent with typical high probability tunneling distances. Closest approach of the  $\text{Na}^+$  ion is taken as 0.1 nm.

### 3.3 Determining the Ion Diffusion Rate

The rate of sodium ion diffusion into defect block surface sites is assumed to be the same as the rate of diffusion into sites within the bulk crystal of the electrolyte, except that there are fewer neighboring sites. The diffusion rate is calculated from the high temperature conductivity of sodium  $\beta$ -alumina, assuming nearest jumps only from second nearest sites or nearest sites. Ionic conduction, diffusion, and ion jump frequency all are activated processes with identical activation energies.

$$\sigma(T) = (\sigma_0/T) \exp(-E/k_B T) \quad [\text{Eq. 3a}]$$

$$D(T) = D_0 \exp(-E/k_B T) \quad [\text{Eq. 3b}]$$

$$\omega = \omega_0 \exp(-E/k_B T) \quad [\text{Eq. 3c}]$$

We derive parameters for high temperature ion diffusion using equations from Sato which relate conductivity, diffusion, and attempt frequencies:

$$\sigma_0 k_B / C = (1/3)(Ze)^2 n d^2 \omega_0 \quad [\text{Eq. 2.2, Sato, ( )}]$$

$$D_0 = C/(Z^2 e^2 n) \quad [\text{Eq. 2.4, Sato, ( )}]$$

Physical parameters for the activation energy averaged from several measurements,  $(E) = 2.6284678 \times 10^{-20} \text{ J/ion}$  and the pre-exponential for conductivity  $\sigma_0 = 3 \times 10^4 \text{ K/(ohm-cm)}$ , given by Moseley. [Moseley] Because  $C = \sigma_0 k_B$ , then  $C = 4.14162 \times 10^{-7} \text{ J/(ohm-m)}$ . The charge on the diffusing ion,  $Ze = 1.602 \times 10^{-19} \text{ C/ion}$ ; the number of diffusing ions per volume of solid electrolyte,  $n = 6.494 \times 10^{27} \text{ Na}^+ \text{ m}^{-3}$ . The jump distance for the diffusing ions,  $d = 0.32389 \times 10^{-9} \text{ m}$  between pairs of Beavers-Ross sites or between mid-oxygen sites. Then  $D_0 = 2.485 \times 10^{-6} \text{ m}^2/\text{s}$ . The attempt frequency for diffusion,  $\omega_0$ , is obtained from Eqs. [2.2] and [2.4] using  $\omega_0 = 3D_0/d^2 = 7.11 \times 10^{13}$ , allowing the single jump frequency to be calculated as a function of temperature.

### 3.4 Probability of electron tunnelling from the electrode

The work function of the alkali metal-coated electrode is fairly low; the Fermi

level itself is raised because of surface states, which may be described possibly too simply as oriented dipoles with the negative pole inside the electrode surface and a positive pole ( the alkali ion ) on the external surface of the electrode, due to alkali metal adsorption on the metal electrode surface. The reaction probability,  $P$ , for electron tunneling to a sodium ion at distance  $a$  in a defect plane edge is described using as a model a simple rectangular potential barrier with a height above the Fermi level equal to the electrode's work function,  $\Phi \approx 2.5 \text{ eV} = 4.00 \times 10^{-19} \text{ J}$ , for a Mo or W alloy electrode covered with a partial monolayer of Na. [ **15. R. Morin, *Surf. Science*, 1 S5, 187 (198S) and V. Medvedev, A. Naumovets, and A. Fedorus, *Soviet Phys.-Solid State* 12, 301 (1970)**] and the total barrier energy is the Fermi energy plus the work function  $V = \Phi + E_F$ . The probability  $P$  is given in Eq.2a: [12]

$$P_T \approx 16E_e(V-E_e)V^{-2} \exp[-4\pi a(2m_e(V-E_e))^{1/2}/h] \quad [\text{Eq. 4}]$$

The electron's energy is  $E_e \approx E_F$  (the Fermi energy) =  $3.05675 \times 10^{-18} \text{ J}$ ; where  $k = 1.38 \times 10^{-23} \text{ J/K}$  is Boltzmann's constant; and as a result  $V = \Phi + E_e \approx 3.45675 \times 10^{-18} \text{ J}$ . The electron mass is  $m_e = 9.1 \times 10^{-31} \text{ kg}$ ; and Planck's constant:  $h = 6.626 \times 10^{-34} \text{ J-s}$ . It is necessary to integrate expression over energies close to the Fermi level, times probability of those energy states being filled (*Fermi-Dirac distribution function*), with number of states and velocity of electrons in states per increment of energy corrected for their dependence on energy.

### 3.5 Sodium Ion/Atom Reorganization Term in Tunneling Probability

The binding energy of the  $\text{Na}^+$  ion to the  $\beta$ "-alumina surface is known, and the equilibrium distances of  $\text{Na}^+$  ion and the  $\text{Na}^0$  atom to the  $\beta$ "-alumina surface may be estimated. We make a rough estimate of the binding energy of the  $\text{Na}^0$  atom to the  $\beta$ "-alumina surface. We can also construct what should be fairly reasonable simple potential energy vs. distance diagrams for these the ion and the atom on the  $\beta$ " surface, because we can describe the attractive term in the ion's case as a ion-ion or an ion-dipole interaction, and in the atom's case as an induced dipole-ion or an induced dipole-dipole interaction,

Since the binding energy of sodium ions to  $\alpha$ -alumina single crystals is known, and the expected sodium ion-oxygen ion distance may be estimated, the potential well is first constructed from the sum of attractive potential going as  $r^{-1}$  and a Lennard-Jones repulsive potential going as  $r^{-12}$ . The potential well is approximated to a harmonic oscillator which will give the same potential difference when a  $A_d = 0.0888 \times 10^{-9} \text{ m}$  occurs. Because the appropriate vibrational excited states are highly excited, and the vibrational energy levels of a  $\text{Na}^+$  bound to the  $\beta$ "-alumina surface are relatively close together, the occupation of vibrational states is treated as if it were continuous Boltzman distribution.

$$\omega = \omega_c \exp(-E/R_g T) \quad [\text{Eq. 13}]$$

The classical frequency for a harmonic oscillator is  $\omega_c$ : where  $V(x) = (1/2)Kx^2 = K(0.3943 \times 10^{-20} \text{ m}^2)$ , and  $K = 18.723855 \text{ J/m}^2$  (from the potential well) which result in  $\omega_c = 2.215 \times 10^{13} \text{ s}^{-1}$ , classical harmonic oscillator frequency,

$$v(x) = 1/2(Kx^2);$$

$$K = 2V(x)x^2;$$

$$\omega_c = (K/m_{\text{Na}^+})^{1/2}; \quad [\text{Eq. 14}]$$

$$\hbar(\text{hbar}) = h/2\pi = 1.054497 \times 10^{-34} \text{ J-s};$$

$$E_n = (n + 1/2)\hbar \omega_c;$$

$$P(E_n) = \exp[-E_n/kT] / \sum_{j=0}^{\infty} \exp[-E_j/kT];$$

The kinetic energy of a classical harmonic oscillator becomes zero at maximum extension, for example of a stretching bound particle. So at maximum extension,

$$\omega_c = 2.215 \times 10^{13} \text{ s}^{-1}$$

$$V(X) = 1/2(Kx_{\text{max}}^2) = E_n = (n + 1/2)\hbar \omega_c, \quad x_{\text{max}} = (2E_n/K)^{1/2}$$

$$\hbar(\text{hbar}) = h/2\pi = 1.054497 \times 10^{-34} \text{ J-s}, \quad E_n = 2.3357109 \times 10^{-21} (n + 1/2)$$

For the  $\text{Na}^0\text{-}\beta$  surface, the binding energy is about 97.6 kJ/mol or  $16.2 \times 10^{-20} \text{ J/atom}$ , and the values of  $K_{\text{Na}^0} = 10.05 \text{ J/m}^2$ ;

$$E_b = 16.2 \times 10^{-20} \text{ J/Na}$$

$$E_b = 97.6 \text{ kJ/mol}$$

$$\omega_{c_{\text{Na}^0}} = 1.62 \times 10^{13} \text{ S}^{-1};$$

$$E_n(\text{Na}^0) = 1.711 \times 10^{-21} \text{ J}(n + 1/2)$$

$$m_{\text{Na}} = 3.817 \times 10^{-26} \text{ kg}; \text{ mass of sodium atom}$$

$$A_{\text{Na}} = \pi/4 (3.7157 \times 10^{-10} \text{ m})^2 = 10.84 \times 10^{-20} \text{ m}^2$$

The desorption of  $\text{Na}^+$  ions deposited on sodium  $\alpha$ -alumina of composition  $\text{Na}_2\text{O} \cdot 8(\text{Al}_2\text{O}_3)$  cut along the a-c plane show several peaks corresponding to a variety of energies, with the second lowest energy, and most prominent peak at 2.18 eV. [15] A lower energy peak at 1.68 eV exists but is very insignificant compared with the larger peak, especially at higher rates. [15]

Then the energy for a 0.0888nm stretch necessary to put the sodium ion at the same distance from the surface as the sodium atom is  $E_{\text{str}} = 44.46 \text{ kJ/mole}$  for 0.0888nm displacement,

### 3.5 Properties of the Electrode and Tunneling Attempt Frequency

Tungsten and molybdenum have body centered cubic crystal structures, with two atoms and 12 valence shell electrons in unit cells with  $a \approx 3.15 \text{ \AA}$ . In operation of electrodes in alkali metal vapor, these electrodes are covered with a partial monolayer of adsorbed alkali metal atoms. The work function of the alkali metal-coated electrode is fairly low. We will use expressions for the density of occupied states and electron collision frequency based on the free-electron model; although transition metals are generally not considered well described by the free electron model, W and Mo are among the most conductive transition metals, and their low temperature electronic contributions to the heat capacity: 1.3 and 2.0 mJ/(mol-K<sup>2</sup>), respectively, compared with calculated values of 1,112 and 1,099 mJ/(mol-K<sup>2</sup>). [Kittel] The electron kinetic energy related to electron velocity is calculated. The tunneling attempt frequency,  $X_e(\epsilon)$ , is calculated from the electron velocity,  $v(\epsilon)$ , the density of states,  $D(\epsilon)$ , and the Fermi-Dirac distribution function,  $F(\epsilon)$ , where  $\epsilon$  is electron energy.

The density of states at the Fermi level, calculated using a free electron model is fairly high. The equations used to determine the relevant parameters are from Kittel, and Table I gives the parameters used to determine the tunneling probability for W and Mo. [Kittel] The Na<sup>+</sup> ion density in BASE is also fairly high in electrochemically active BASE grains. As a result, these probabilities along with the reactant/product densities and the observed lack of significant activation energy, except for the activation energy associated with alkali metal evaporation, strongly support the tunneling model and suggest the BASE defect block edge as the reaction site. Additionally these observations suggest that the reaction occurs primarily close to the three phase contact line.

The Fermi-Dirac distribution function gives the occupancy of states as a function of energy and temperature. Multiplied by the density of states function,  $D(\epsilon)$ , gives the density of occupied states. Tunneling occurs when the initial and final state have similar energies. The Na<sup>+</sup>/Na<sup>0</sup> electrochemical couple is in equilibrium with the chemical potential of the electrode, although individual ions and atoms also will show a distribution of energy levels. The energy at the Fermi level,  $\epsilon_f \approx \mu$ , the chemical potential at temperatures which are not extremely high.

$$F(\epsilon) = 1/(1 + \exp[(\epsilon - \mu)/k_B T]) \quad [\text{Eq. 6}]$$

$$\mu \approx \epsilon_f = \hbar^2/2m_e (3\pi^2 N/V)^{2/3} \quad [\text{Eq. 7}]$$

for Mo

$$\begin{aligned} d &= 2.725 \times 10^{-10} \text{ m} \\ a &= 3.1467 \times 10^{-10} \text{ m} \\ V &= 31.157 \times 10^{-30} \text{ m}^3 \\ N/V &= 0.38515 \times 10^{30} \text{ valence electrons/m}^3, \\ \text{atoms/m}^3 &= 3.20955 \times 10^{28} \\ \epsilon_f &= 3.0922993 \times 10^{-18} \text{ J;} \\ v(\epsilon_f) &; 2.6056617 \times 10^6 \text{ m/s} \\ D(\epsilon_f) &= 1.868252 \times 10^{-47} \text{ J}^{-1} \text{ m}^3 \\ X_e(\epsilon_f) &= 7.0264 \times 10^{-52} \text{ (m}^2\text{-s-J)}^{-1} \end{aligned}$$

The velocity of electrons at Fermi level (or near the Fermi level) is directly calculable from the kinetic energy of the conduction electrons.

$$v(\epsilon) = (2\epsilon/m_e)^{1/2} \quad [\text{Eq. 8}]$$

In order to find the collision rate of electrons with the electrode surface, the total velocity is divided by  $2\sqrt{3}$  to determine the velocity component perpendicular to the electrode edge of those electrons traveling toward the edge, and the density of states is multiplied by the Fermi function to give the number of filled states. The Fermi function is 1/2 at the Fermi energy, Because the  $\text{Na}^+/\text{Na}^0$  electrochemical couple is in equilibrium with the Fermi level of the metal, tunneling can take place, but only electrons within about  $\pm k_B T$  of the Fermi energy can contribute, because the initial and final states must have the same energy, so that in the final state the adsorbed sodium atom has an energy between 0 and  $2k_B T$  above its lowest energy state. (Electrons at higher energies could contribute but there are not enough of them to change the result.)

$$X_e(\epsilon) = (v(\epsilon)/2\sqrt{3}) * D(\epsilon) * F(\epsilon) \quad [\text{Eq. 9}]$$

We are counting collisions of electrons within  $\pm k_B T$  of  $\epsilon_f$ . The number of collisions by electrons in this energy range.

$$\int_{\epsilon_f - k_B T}^{\epsilon_f + k_B T} X_e(\epsilon) d\epsilon \approx X_e(\epsilon_f) \times 2 \times k_B \times 1/2 \times 1000 \text{ K} = 9.70 \times 10^{32} / (\text{m}^2\text{-s}) \quad [\text{Eq. 10}]$$

The total reaction rate is determined from the tunneling rate and the resorption / adsorption rate,  $X_{Na}$ , occurring sequentially. The latter controls the rate close to the three-phase interface, and is not dependent on the integration variables. The integrated rate with respect to distance is most conveniently integrated using conical coordinate about a normal to the plane of the electrode surface.

The product of the tunneling probability,  $P_T(x, r, \epsilon)$ , with an attempt frequency,  $W_e(\epsilon)$ , for electrons near the Fermi level “colliding” with the electrode surface, integrated over the distance between the electrode and  $\text{Na}^+$  sites, and over the occupied energy states in the electrode, gives the overall tunneling rate,  $K_T(x, r, \epsilon)$ . The number of occupied energy states as a function of energy is given by the product of the Fermi-Dirac distribution function,  $F(\epsilon)$  and the density of states,  $D(\epsilon)$ . The attempt frequency,  $W_e(\epsilon)$ , is calculated from the velocity of electrons at the Fermi level, the density of states, and the occupancy of states given by the Fermi-Dirac distribution function,

Calculation of a reaction rate from Eq. 2a requires that estimates of the densities of states from which the electrons tunnel, and the density of  $\text{Na}^+$  ions on the surface of the solid electrolyte, which are the electron acceptors to which the electrons tunnel. The value of the reaction rate is taken to be the product of several terms. The tunnelling attempt frequency, is itself a product of the free electron collision for electrons close to the Fermi level, the Fermi function which gives the temperature dependent part of electron density, and the density of states at the Fermi level. The density of  $\text{Na}^+$  occupied surface sites on the BASE defect block surface; and the transmission probability,  $P$ , have been described above. [13] The tunneling rate is therefore  $K_T(\mathbf{F}, \mathbf{r}, \mathbf{x})$ :

$$K_T(\epsilon, \mathbf{r}, \mathbf{x}) = (W_e(\epsilon, \mathbf{r}, \mathbf{x}) (d_{\text{Na}^+}(\mathbf{x})) (P_T(\epsilon, \mathbf{r}, \mathbf{x})) d\epsilon, d\mathbf{r}, d\mathbf{x} \quad [\text{Eq. 11}]$$

### 3.6 Solving the Integral

The integral which gives the total reaction rate is calculated by evaluating at discrete points over the two conical spatial coordinates and the energy coordinate. This calculation is designed to carry out a triple integral over two spatial coordinates,  $x$  and  $r$ , in conical coordinates, and over energy, from  $\epsilon_F - k_B T$  to  $\epsilon_F + k_B T$ , to compute the exchange current of an AMTEC electrode.

$$J_0^0(T) = \int_{-1}^1 \int_0^\pi \int_{\epsilon_F - k_B T}^{\epsilon_F + k_B T} (1/K_T + 1/X_e(\epsilon_r))^{-1} d\epsilon, d\mathbf{r}, d\mathbf{x} \quad [\text{Eq. 12}]$$

The total rate integral can apparently be solved in closed form only if the electrode area providing tunneling electrons is fixed. This is an unrealistic assumption. The integral is most readily and precisely evaluated numerically over two conical spatial coordinates,  $x$  and  $r$ , and one energy coordinate,  $e$ .

The innermost integral calculates the rate contribution over energy, calculating electron velocity, collision frequency, and tunneling probability with respect to energy, and evaluating these quantities from  $\epsilon = \epsilon_F - k_B T$  to  $\epsilon = \epsilon_F + k_B T$  in steps of  $k_B T/10$ .

integrating over energy is not necessary to obtain fairly good accuracy, as it may be approximated by assuming that there are  $2k_B T * D(\epsilon_F) * F(\epsilon_F)$  electrons

at the Fermi energy  $\epsilon_F$ , with velocity  $v(\epsilon_F)$ , and with a collision frequency of the electrons with the electrode surface,  $X_e(\epsilon_F)$ . The Fermi-Dirac distribution function,  $F(\epsilon) = 1/(1 + \exp[(\epsilon - \mu)/k_B T])$ , where the chemical potential,  $\mu$ , is almost exactly equal to the Fermi energy,  $\epsilon_F$ , at temperatures below several thousand K, and therefore  $F(\epsilon_F) = 0.5$ .

The outermost integral steps over the distance from the three-phase line,  $x$ , from the distance of closest approach, 0.1 nm to about 2.0 or 3.0 nm in steps of 0.01 to 0.05 nm.

The intermediate integral steps from  $r = 0.0$  to  $r = 2.0$  nm in steps of 0.1 nm over the radial spatial coordinate,  $r$ , about the intersection of a normal to the electrode surface to the BASE area element at distance,  $x$ .

It also calculates the area of the ring-like area element from  $r$  to  $r$  plus  $\Delta r$  and at constant distance from the BASE area element. The ring is truncated at the three-phase boundary. Therefore its area depends on the value of  $r$  and  $\Delta r$ , and also on the distance above the three-phase boundary of the intersection of the normal to the electrode from the BASE segment.

### 3.7 Effect of electron hopping along defect block on reaction rate

We will compare this rate to the rate of a evaporation of the bound sodium atom or ion, in order to determine how far out from three phase line electron hopping can occur before the probability of evaporation overwhelms the probability of hopping. Hopping cannot occur efficiently between adjacent defect blocks because the distance is about 1 nm and only about 2 sites are close enough to the site on the adjacent defect block to be within the 1.1-1.2 nm range for very low probability tunneling. It is also necessary to determine the stretching distance and rearrangement energy which must occur for a bound sodium ion before an electron from a neighboring sodium atom can tunnel to it. The distance between occupied sites is typically  $d_{2h} = 0.32389 \times 10^{-9}$  m, while the distance for a stretch which brings the sodium ion to the approximate equilibrium position of an adsorbed sodium atom is  $d_{str} = 0.0888 \times 10^{-9}$  m, ( $\text{Na}^+$  rearrangement stretch).

The transition probability for vibrationally excited states of the sodium ion to states of the sodium atom were discussed above in section 3.4A

The following calculation is correct for the transition from the single optimally vibrationally excited state of the sodium ion on BASE to the the equilibrium state or excited states of the bound sodium atom. There are about thirty other vibrationally excited states of the sodium ion on BASE which make lesser contributions to the overall tunneling probability.

We can expect that the vibration necessary for electron hopping will occur

several orders of magnitude faster than desorption, However tunneling can only occur if one state is filled and the other empty. The chemical potential, determined by the activities of  $\text{Na}^+$  and  $\text{Na}^0$  in the BASF, is in equilibrium with that in the porous electrode, (which tells us nothing about their surface concentrations) so the work function of the electrode is equal to the tunneling barrier for electron tunneling from  $\text{Na}^0$  to  $\text{Na}^+$  on the defect block surface.

If first site jumps and second site jumps are both allowed and equally common, we would expect about 314 jumps before desorption occurs. In fact, site occupancy is always less than 1.0, and there may not be space for  $\text{Na}^+$  and  $\text{Na}^0$  to occupy sites 0.24 nm apart, so nearest site jumps may not occur. Electrostatic repulsion should tend to keep two  $\text{Na}^+$  ions from occupying adjacent sites. If only second site jumps are allowed, we can expect only about 43 jumps, or 21 nm maximum hopping distance, before desorption occurs. The most likely physical picture is first and second site jumps mixed with third site jumps. A few larger jumps would not be important for the following reasons. (1) A mechanism for a four site jump with intervening  $\text{Na}^0$  can occur via two second site jumps, at time equal to the sum of two second site jumps, (2) The migration of a  $\text{Na}^+$  to the defect block surface segment containing three sequential vacancies will occur much faster than hopping. Because of these reasons, jumping over two vacant sites is the lowest frequency process we need to consider within the defect block, and hopping between defect blocks is clearly not important. The radius of the  $\text{Na}^+$  ion,  $r_{\text{Na}^+} = 0.097 \times 10^{-9} \text{ m}$ , and the radius of the sodium atom is  $r_{\text{Na}} = 0.186 \times 10^{-9} \text{ m}$ , indicating that they probably will not reside on adjacent sites unless bond formation occurs. Hopping between adjacent defect blocks will occur much less frequently than desorption, and may be ignored, except perhaps in the case of defect blocks parallel to the 3-phase boundary, where large numbers of filled states on one block and unfilled states on the more distant block exist to allow occasional electron transfer. If the defect block has a regular structure, we can expect about half the total BR and mid-oxygen sites (we count the pair of m.o. sites as one site) to be occupied, with the remaining sites filled predominately with more strongly bound  $\text{Na}^+$  and the remainder with less strongly bound  $\text{Na}^0$ . We will arbitrarily assume 1/3 of the sites are vacant, 1/2 have  $\text{Na}^+$  ions, and 1/6 have  $\text{Na}^0$ . However, if an electron hops to a sodium ion adjacent by  $0.32389 \times 10^{-9} \text{ m}$  to a sodium atom with another sodium ion adjacent to it, the probabilities of the disposition of the two electrons after one hop of each sodium atom's valence electron is identical to that if the two valence electrons did not effect each other, assuming hops of only two sites occur. Therefore the random walk calculation is carried out for a regular sequence of sodium ions each separated by two sites from their neighbors.

There will be about one  $\text{Na}^0$  in the first 1.2 nm reaction zone away from the three-phase line, but we will carry out the calculation to determine the disposition of one electron associated with one  $\text{Na}^0$  at 1.0 nm in the reaction zone.



At the stationary state, no gradient exists, so the problem becomes a random walk, with  $U(x,t)$  giving the probability that the electron has travelled to point  $x$  in time  $t$ .

$$U(x,t) = 1 / (2\pi t)^{0.5} \exp[-x^2/2t] \quad [\text{Eq. 15}]$$

We also assume that electrons which hop to the three-phase line tunnel to the electrode, instead of being reflected, but that the rapid tunneling within the first nm maintains the  $\text{Na}^0$  concentration in this regime, so that the concentration of  $\text{Na}^0$  at the edge of the reaction zone does not decrease. On average, at 10(K)K, the electron associated with  $\text{Na}^0$  can only hop for  $2.16 \times 10^{-8}$  s before desorbing; but each hopping step occurs once in  $3.??? \times 10^{-10}$  s, so 61.6 random hops are possible.

This allows on average 61.6 jumps for a maximum travel of 19.92nm before resorption, and average random travel of 1.927nm, effectively multiplying the overall reaction rate by about  $2.93 = (1.0 + 1.93)$ , for defect blocks perpendicular to the 3-phase interface.

For an average orientation of defect block at 45 degrees to the 3-phase boundary, instead of the perpendicular defect block we have been considering so far, results in hopping away from the 3-phase boundary for an additional 1.31 nm beyond the direct reaction zone, if a  $\text{Na}^0$  gradient exists. The average direct tunneling reaction zone is about 1.55nm long, so that the total reaction zone is multiplied by  $2.86/1.55$ .

#### 4. DISCUSSION

There are several sources of uncertainty in the model as well as several physical] y reasonable processes which might affect the rate but for which there is no available experimental or theoretical basis for quantitative assessment, The sources of uncertainty are:

1. Morphological parameters
  - 1.1 Length of three phase interface
  - 1.2 Contact angle between electrode and solid electrolyte
  - 1.3 Area of electrochemically active solid electrolyte
  - 1.4 Density of defect blocks on electrochemically active areas on BASE
2. Binding energy of Na to BASE surface has not been directly measured but estimated to be close to binding energy of Na atoms to Na bulk, probably somewhat lower resulting in faster adsorption / dcsorption. This will be discussed in detail below.
3. Does the apparently fast (compared with adsorption/desorption) diffusion of  $\text{Na}^+$  to/from the reaction site need to be included. Does a vibration associated with the sodium moving from the position favorable for an ion to that for the larger neutral atom need to be considered? It also should be a very fast process.
4. Since the Mo electrode is coated with Na, the Fermi level is raised, and we use a simple free electron model to compute "attempt frequency" for electron transfer from the metal to the sodium ion. Mo and W are among the closest to free electron metals of transition metals, based on high conductivity and on the electronic component of thermal conductivity, which agrees rather well with that calculated for six free electrons per atom,

It is possible that there may be a minimum approach distance, on the order of perhaps 0.1 to 0.2 nm, which occurs in the actual system. However it is also possible that some asymmetry exists for this reaction even though it is not reflected in an clear deviation of the transfer coefficient,  $\alpha$ , from a value of 0.5. Reduction of  $\text{Na}^+$  may occur under the electrode grains to some extent, and while  $\text{Na}^+$  would be expected to be absent, or strongly bound on BASE surfaces away from the defect block, Na atoms may diffuse on BASE to the reaction zone.

For accurate assessment of the exchange current, it will be necessary to include the accurate functional dependence of each parameter in the rate equation on alkali metal activity. These parameters have been usually approximated as constants,

Adsorption of  $\text{Na}^0$  on BASE

Wetting characteristics and interracial resistances which indicate interface characteristics of liquid sodium on BASE suggest a weak attractive interaction at higher temperatures and a weak

repulsion at lower temperatures. Only coverage fairly close to the three phase line (within several run) is important, as tunneling rate drops off rapidly with distance, and it doesn't matter if we underestimate the tunneling rate at close in distances where the evaporation rate controls the rate because it's so much lower than the tunnelling rate. Since the Na atom and either K or the K atom has a diameter about as large as the defect plane, and the coverage is about 0.5 or perhaps a little lower, we take  $\theta = 0.5$ , neglecting surface states further removed from the defect block intersection with the 3-phase line. The binding enthalpy of the sodium atom to the BASE surface is a good example of an estimate, taken to be equal to the heat of evaporation of liquid sodium, which was made with some experimental and theoretical justification, in the absence of quantitative measurements. The heat of vaporization of an atom of sodium in the liquid phase equals the total enthalpy change when a sodium ion is separated from an electron in the liquid sodium reservoir at T<sub>2</sub>, travels through the  $\beta$ -alumina, recombines at the exterior electrode with the electron, and escapes into the gas phase as a neutral atom, [Vining] Much of the AMTEC literature implies that the enthalpy of the last process is essentially equivalent to the heat of vaporization, although this is not required from thermodynamic considerations alone. [DeJonghe,] However, thermal characterization of the AMTEC cell has been carried out, and has detected no indications of unusual heats associated specifically with the transfer of the sodium atom at the BASE surface to the gas phase. [Expand and reference: Ryan] Calculations of the nature of sodium atom binding to the  $\beta$ -alumina surface have been carried out. [Expand and refer] Neutral Na isotherm on BASE should be measured.

Furthermore, the absence of appropriate energy levels in BASE capable of accepting electrons from an adsorbed sodium atom, or surface atoms which could readily expand their coordination number to form covalent bonds to the adsorbed atom both indicate that the adsorption is weak and nonspecific. This reasoning does not immediately lead to the conclusion that the adsorption energy is equivalent to the heat of vaporization of the liquid, but does suggest that the adsorption energy should not be much greater and could in fact be significantly less.

When the observation of good wetting of BASE by liquid sodium at elevated temperatures is also considered, we arrive at the conclusion that the sodium-BASE interaction is not significantly weaker than the sodium-sodium interaction, and find a justification for estimation of the Sodium atom binding energy to the BASE surface to be about the same as the binding energy of the atom to its liquid - the heat of vaporization.

### **Adsorption of alkali atoms on Mo, W, and alloys.**

The low work function on Na or K covered Mo or W is associated with the adsorbed atoms/ions. K tends to behave largely as an adsorbed ion and Na is more similar to an adsorbed atom, although both are neither purely ionic or atomic on the surface. Coverage is probably several tenths of a monolayer at the pressures typical of those used to determine exchange currents, since the binding energy for the first few tenths of a monolayer is about 2.5 times the binding energy at a full monolayer.

The calculations are normalized to unit activity and a full monolayer would exist under these conditions, but this would only increase coverage by a factor of 2 or 3, affecting exchange current minimally, and we do not actually measure exchange currents at that pressure, and can

not because the Faradaic resistive contributions would generally be too small to measure with any accuracy.

Several mechanisms which are physically reasonable could be responsible for the higher value of the exchange current compared with the calculated exchange current:

1. Electron hopping along defect block edges to reduce  $\text{Na}^+$  at much larger distances than would be accessible by direct single step tunneling will significantly increase the overall rate. This process is expected to drop off as evaporation successfully competes with the series of tunneling steps.
2. Rapid surface diffusion of  $\text{Na}^+$  away from defect blocks to cover the surface of the BASE spine blocks would substantially increase reaction area by at least a factor of three to four.
3. Role of boundary between electrode grains and BASE; can sodium diffuse along this grain boundary and would diffusing for 5 nm or so show up in the measured transport? The high frequency exchange current clearly has a contribution from reaction sites that Na can't readily escape.

## 5. CONCLUSIONS

Given the experimental observation that the interracial reaction rate is not activated, and can be accounted for by a reaction zone near the three-phase interface line, the most likely mechanism is electron tunneling from the electrode to a Na<sup>+</sup> ion at the surface of the  $\beta$ -alumina, which involves tunneling through a barrier equal to the work function of the electrode surface ( $\sim 2.5\text{eV}$ ) with a barrier thickness of  $\leq 1.0\text{ nm}$ . The alkali metal atom is therefore produced on the BASE surface and may travel by gas phase diffusion or chemisorb on the metallic electrode and move by activated surface or grain-boundary diffusion.

to end of  
pt

If sodium atom mobility on the surface of BASE is more rapid than the resorption rate, this process will have the same effect as rapid  $\text{Na}^+$  mobility, and will tend to make the effective reaction area equal the entire  $[\text{hk}0]$  surface within the tunneling distance of the porous metal electrode. If both sodium atoms and sodium ions diffuse more rapidly on this surface than the resorption rate, the increase will be determined by the effect of the more rapidly moving species, and the effects will not be additive.

## 7. ACKNOWLEDGEMENTS

The research described in this paper was performed by the Jet Propulsion Laboratory, California Institute of Technology, and was supported by the Caltech President's Fund, the National Aeronautics and Space Administration, and the Air Force ~~Weapon~~ Laboratory.

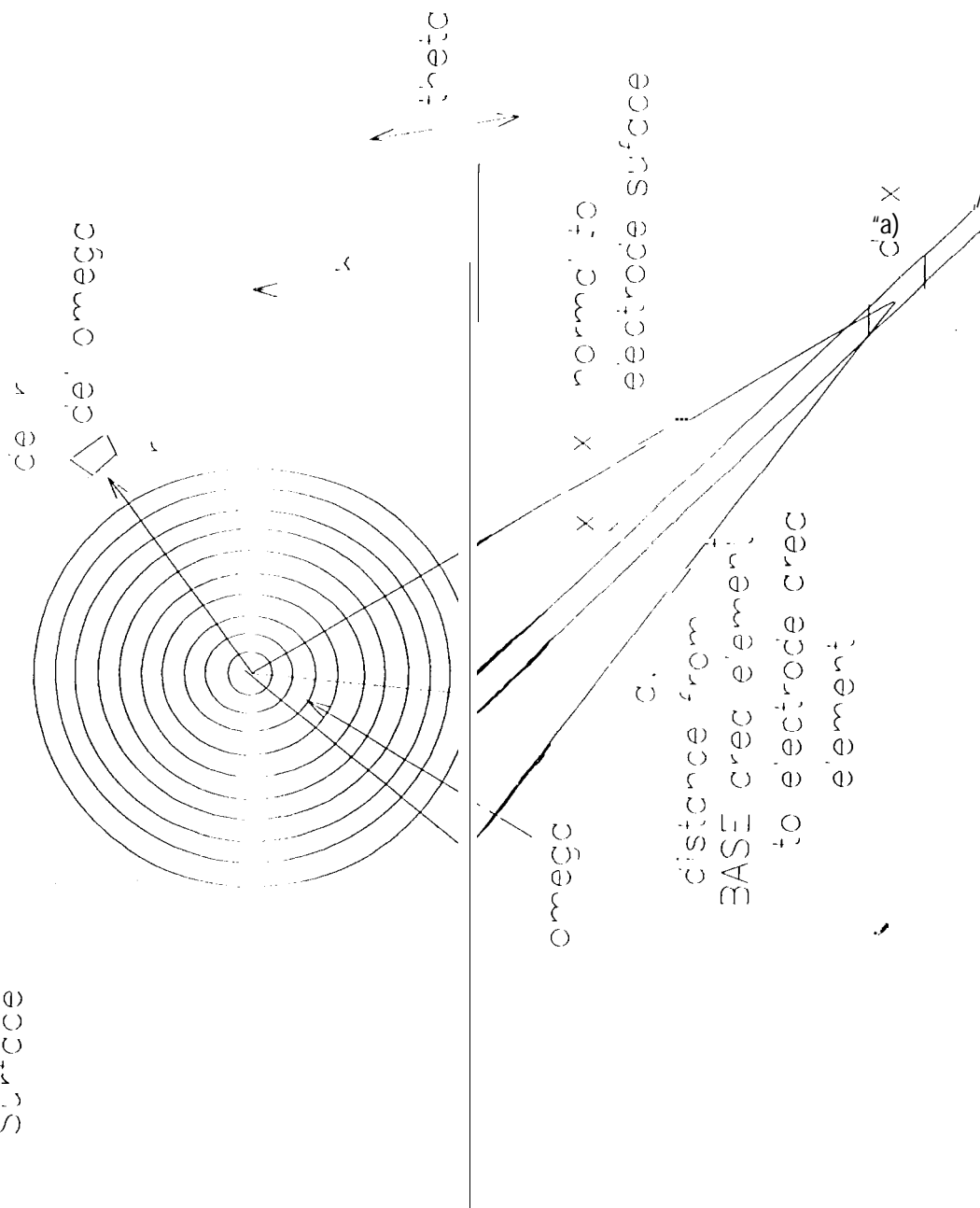
Phillips

## 8. REFERENCES

1. Gurney, R. W., *Proc. Royal Soc. A*, **134**, 137 (1931)
2. Gerischer, H., *Zeit. Phys. Chemie N. F.*, **26**, 223; 325 (1960)
3. R. M. Williams, B. Jeffries-Nakamura, M. L. Underwood, C. P. Bankston, and J. T. Kummer, *J. Electrochem. Soc.*, **137**, 1716 (1990)
4. R. M. Williams, B. Jeffries-Nakamura, M. L. Underwood, B. L. Wheeler, M. E. Loveland, S. J. Kikkert, J. L. Lamb, T. Cole, J. T. Kummer and C. P. Bankston, *J. Electrochem. Soc.*, **136**, 893 (1989)
5. R. M. Williams, M. E. Loveland, B. Jeffries-Nakamura, M. L. Underwood, C. P. Bankston, H. Leduc, and J. T. Kummer, *J. Electrochem. Soc.*, **137**, 1709 (1990)
6. R. Williams, A. Kisor, M. A. Ryan, B. Jeffries-Nakamura, S. Kikkert, and D. E. O'Connor, *29th Intersociety Energy Conversion Engineering Conference Proceedings*, **2**, 888 (1994)
7. L. Schmidt and R. Gomer *J. Chin. Phys.*, **42**, 10 (196S) K on W coverage
8. V. K. Medvedev, A. G. Naumovets, and A. G. Fedorus, *Soviet Phys. - Solid State*, **12**, 301 (1970) Na on W, get this ref.
9. R. Morin, *Surface Science*, **15S**, 187 (1985) work function of W with Na films
10. Z. Li, R. Iamb, W. Allison, and R. Willis, *Surface Science*, **211/212**, 931 (1989) work function of W with K film
11. C. Mail he, S. Visco, and 1.. DeJonghe, *J. Electrochem. Soc.*, **134**, 1121 (1987)
12. R. Williams, B. Jeffries-Nakamura, M. Underwood, D. O'Connor, M. Ryan, S. Kikkert, and C. Bankston, *25th Intersociety Energy Conversion Engineering Conference Proceedings*, **2**, 413 (1990)
13. N. Weber, *Energy Conversion*, **14**, 1, (1974)

14. Lee, Woodrow W. and Choi, Sang-il, "The electronic structure of  $\beta$ -alumina surface with an adsorbed sodium atom", *J. Chem. Phys.*, 72-7, 3884-3888, (1980)
15. M. Knotek, "Study of the thermal desorption of ions from the surface of  $\alpha$ -alumina" *Phys. Rev. B*, 14, 3406 (1976)
16. R. Ditchburn and J. Gilmore, *Rev. Mod. Phys.*, **13**, 310 (1941)
17. U. Buck and H. Pauly, *Z. Phys. Chem.*, 44, 345 (1965)
18. L. I. Schiff, *Quantum Mechanics*, 3rd edition, p 102-104, eq. 17.8, McGraw-Hill Book Co., N.Y., (1968)
19. S. Glasstone, K. Laidler, and H. Eyring, **Theory of Rate Processes**, McGraw-Hill, New York, (1941)
20. **CRC Handbook of Chemistry and Physics**, 68\* Edition, editor in chief, R.C. Weast, pp. F106, F90 CRC Press, Inc., Boca Raton, FL (1987)
21. R. Morin, *Surf. Science*, 155, 187, (1985)
22. L. Schmidt and R. Gomer, *J. Chem. Phys.*, 42, 10, (1965)
23. C. Todd and T. Rhodin, *Surf. Science*, 42, 109 (1974)
24. H. Sato, "Some Theoretical Aspects of Solid Electrolytes" in **Solid Electrolytes** edited by S. Geller, Springer-Verlag, New York, 1977
25. P. T. Moseley, "The Solid Electrolyte" in **The Sodium-Sulfur Battery** eds. J.L. Sudworth and A. R. Tilley, Chapman and Hall, New York, 1985; p44-45
26. Jani, A. R., Tripathi, G. S., Brenner, N. E., and Callaway, J. "Band structure and related properties of Molybdenum", *Phys. Rev. B*, 40 1593-1602 (1989)

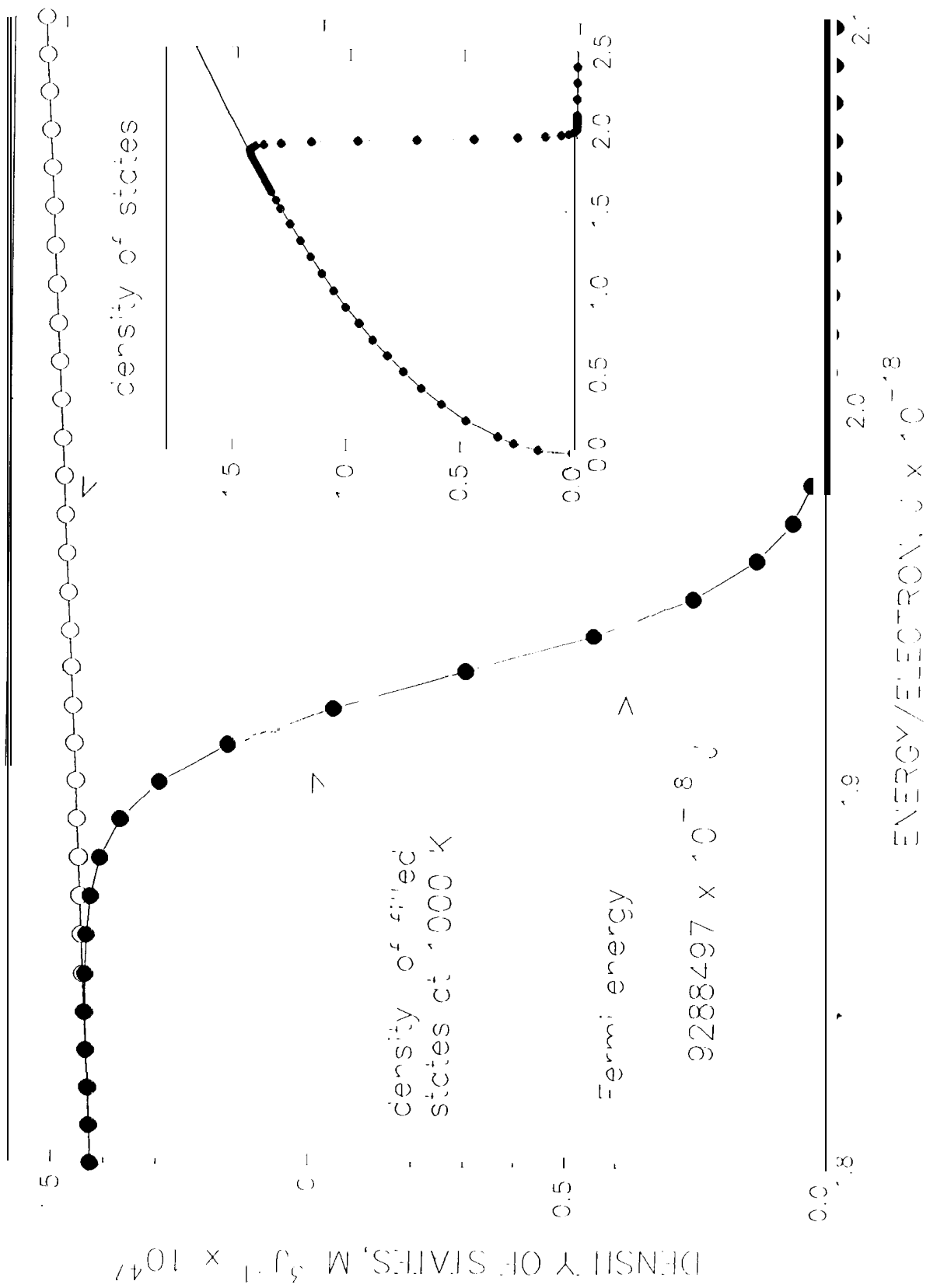
Electrode Surface

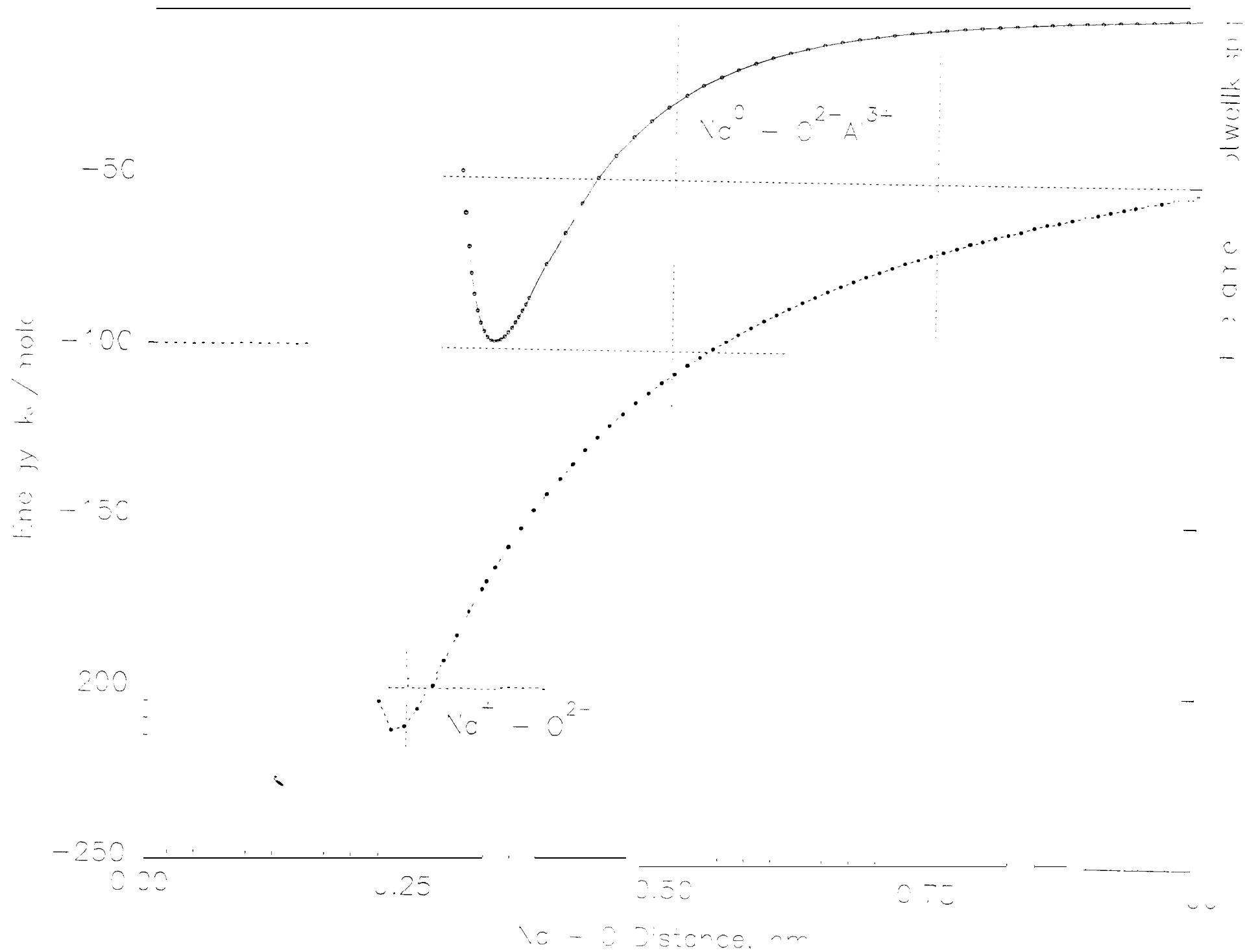


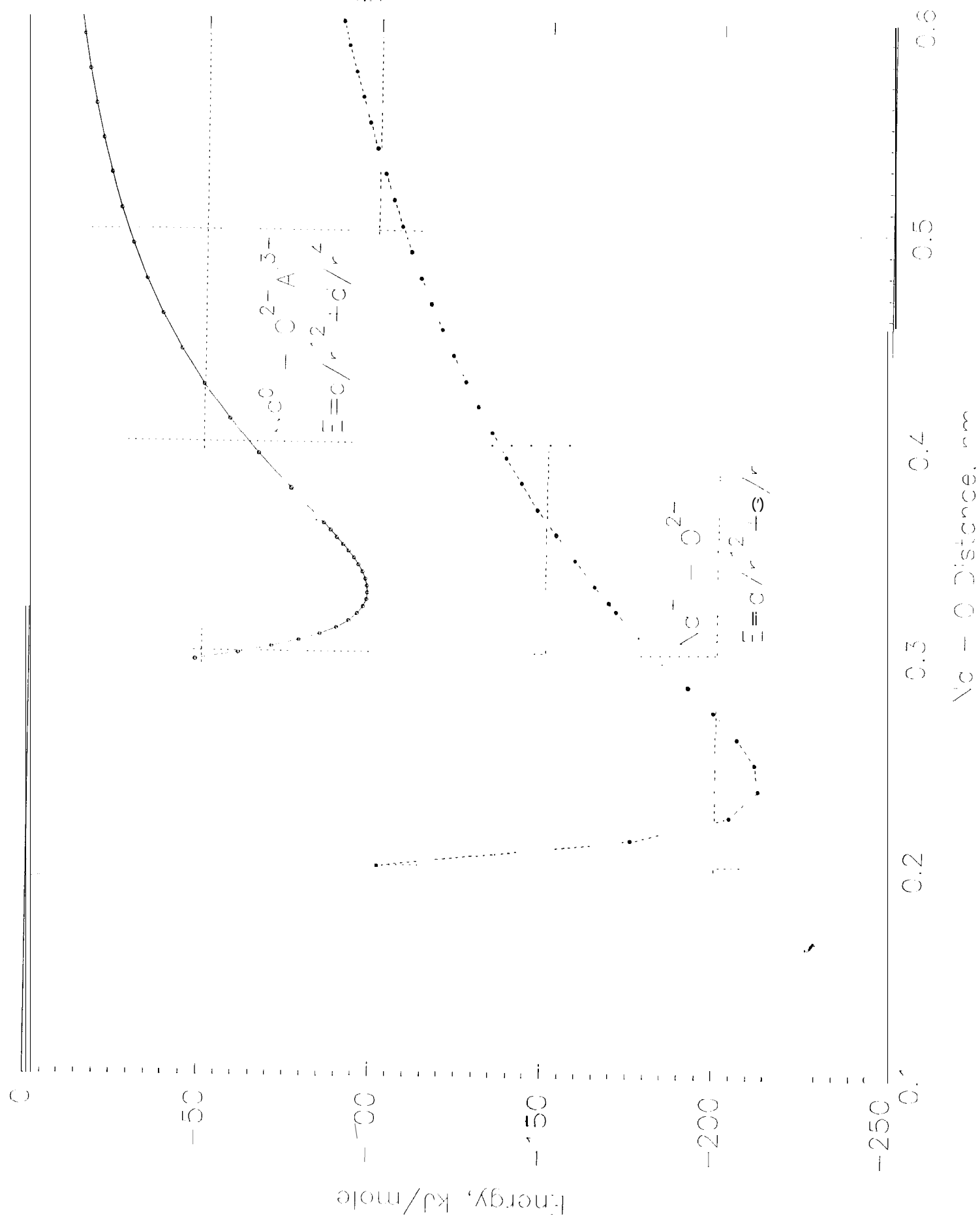
BASE Surface

Figure 1. Conical coordinate system used to calculate tunneling probability from the electrode surface to an area element on the BASE surface.





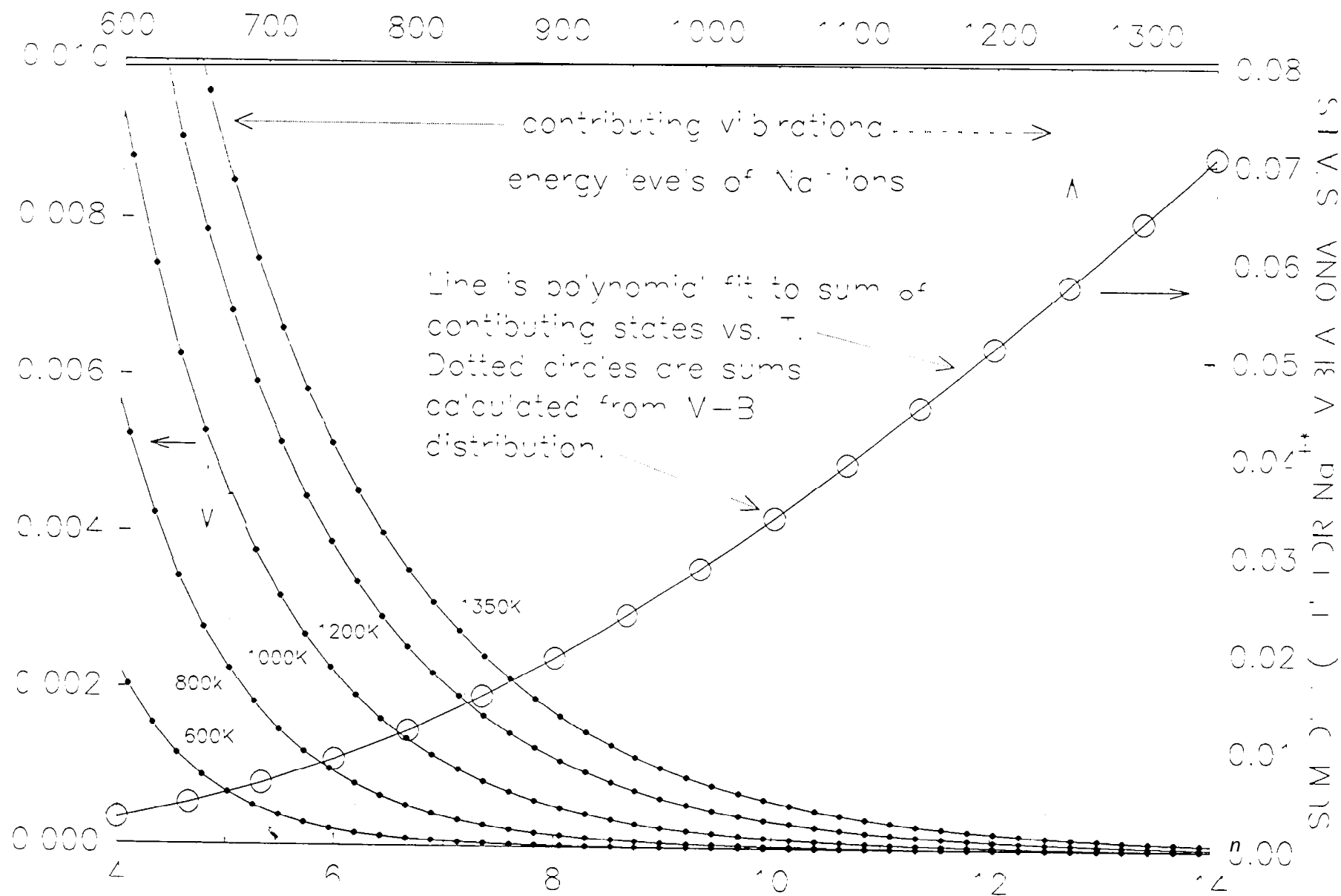




RATIONAL OCCUPANCY OF VIBRATIONAL EXCITED STATES

TEMPERATURE, K

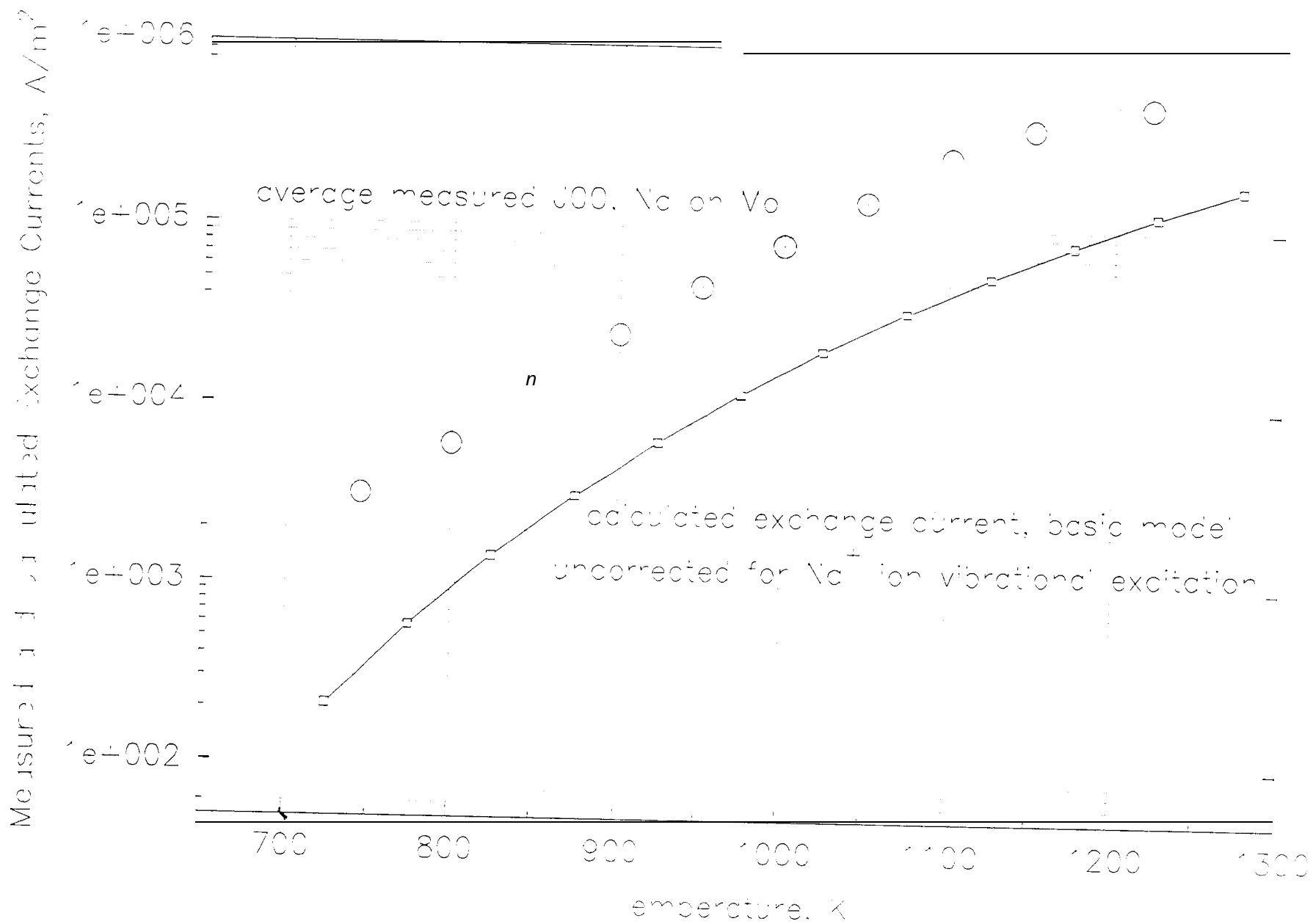
filename = jvbr#3.sc5

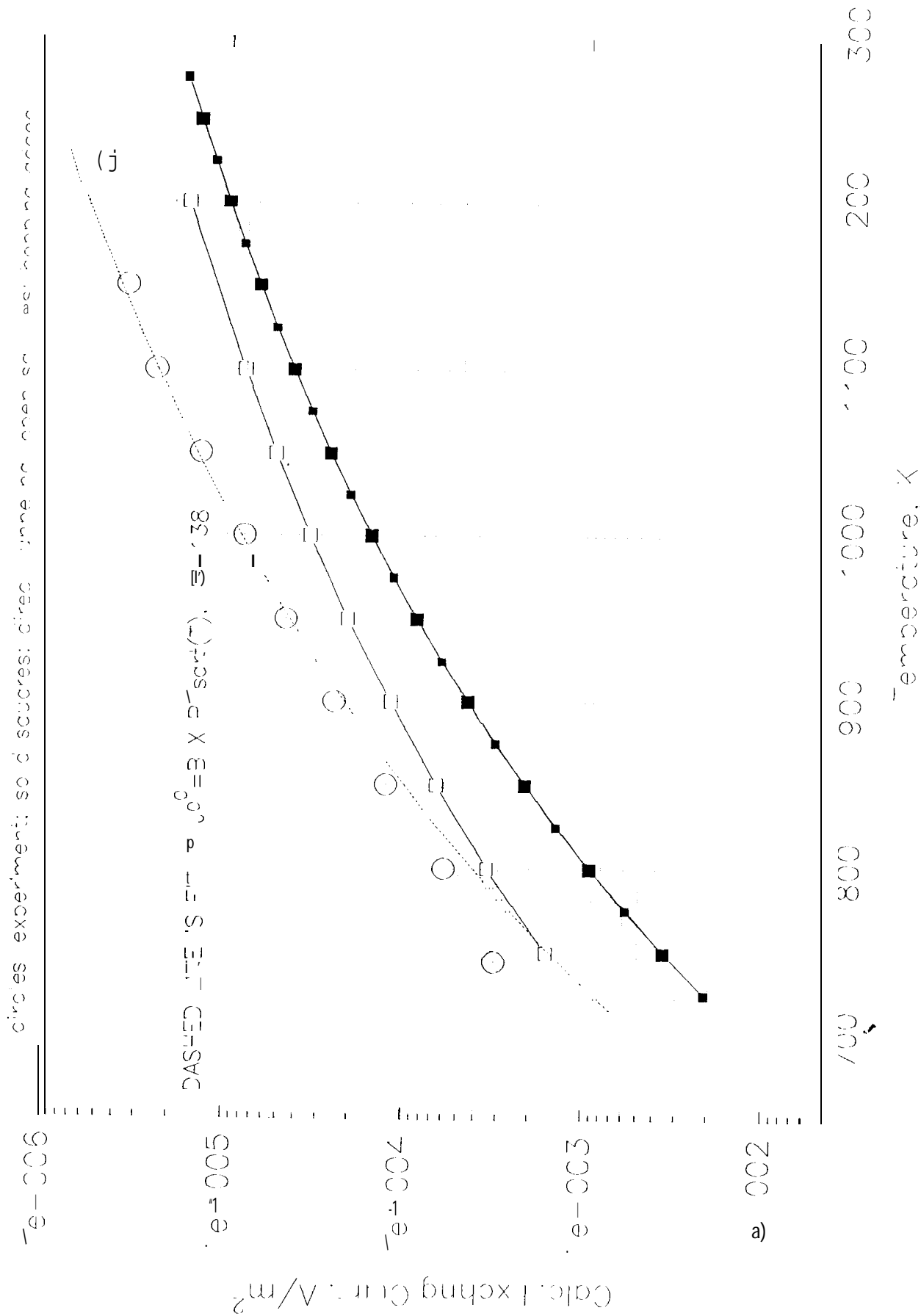


$O_2^+ - Nc^+$  STRETCH VIBRATIONAL ENERGY, per  $Nc^{++}$ ,  $J \times E-20$

$$SUM = A + B \times T + C \times T^2 + D \times T^3 + G/T$$

$A=0.125864; B=-3.06463E-4; C=2.94270E-7; D=-6.66359E-11; G=-18.506$





This preliminary model with hopping includes only one excited vibrational state and no overlap factor; we may expect an average increase of  $\sqrt{30/2}$  or about 4.